Proceedings Eighth Workshop Geothermal Reservoir Engineering
Stanford University, Stanford, California, December 1982
SGP-TR-60

Modeling Studies of the Natural State of the Krafla Geothermal Field, Iceland

Gudmundur S. Bodvarsson*, Karsten Pruess*,
Valgardur Stefansson+, and Einar T. Eliasson[x]

Earth Sciences Division
Lawrence Berkeley Laboratory, University of California
Berkeley, California 94720

Introduction

The Krafla geothermal field is located on the neovolcanic zone in north-eastern Iceland. To date, over 20 wells have been drilled at the site (Figure 1), revealing the presence of high temperature (up to 350°C) geothermal reservoirs. The subsurface rocks are mostly basaltic, with tuffs dominating in the uppermost 800 meters, and subareal lavas and intrusions dominating below 800 m. In the "old" wellfield (west of the gully Hveragil) there are two reservoirs. Below a 200 m thick caprock, there is a compressed liquid reservoir extending to a depth of approximately 1000 m. This reservoir (upper reservoir) contains fluids with temperatures of 200 - 220°C (Figure 2). Below the upper reservoir there is a confining layer at depths of 1000 - 1500 m; the confining layer increases in thickness to the west. The lower reservoir underlies the confining layer and extends to a depth in excess of 2200 m (the depth of the deepest well). It contains a gas-rich steam-water mixture.

In the new wellfield (to the east) the two-phase zone extends practically to the surface, and the temperatures follow the boiling curve with depth.

Prior to the exploitation of a geothermal system, the mass and heat flows in the reservoir are controlled by natural driving forces. The mass transfer is generally dominated by upflow zones, where hot fluids emerge from depth, and by lateral flows that result from the regional groundwater pressure gradients. Geochemical evidence has indicated the presence of three major upflow zones at Krafla, the first one in the Leirhnjukur area (west of the old wellfield), the second one in the "old" wellfield close to Hveragil, and the third one in the "new" wellfield (Armannsson, Gislason and Hauksson, 1982). The latter two upflow zones control the natural flows as conceptualized in the model shown in Figure 2 (Stefansson, 1982).

A gas-rich steam-water mixture flows from the west in the lower reservoir in the old wellfield, and rises through a fracture zone near Hveragil, where it mixes with fluids from the reservoir in the new wellfield. Most of the noncondensible gases and some of the fluids discharge at surface manifestation in Hveragil, but the rest recharge the upper reservoir in the old wellfield. In the new wellfield a steam-water mixture rises through an upflow zone, moves laterally to the west towards Hveragil and mixes with fluids from the lower reservoir in the old wellfield. Some of the fluids in the reservoir in the new wellfield are discharged to the surface as evidenced by surface manifestations there.

In modeling the Krafla reservoir in its natural state, all of the major physical processes that take place in the reservoir must be considered. These include mass transport, conductive and convective heat transfer, and boiling and condensation. The major objectives of the present work are:

1) To verify a conceptual model of the field.

2) To resolve the mechanism that controls the low temperatures in the upper reservoir, which is recharged by fluids of much higher temperatures.

3) To quantify natural mass and heat flows in the reservoir.

4) To verify permeability values obtained from the analysis of injection test data.

5) To obtain a better understanding of the dynamic nature of the reservoir; i.e., set the background for further reservoir modeling studies.

* Lawrence Berkeley Laboratory, Berkeley, California
+ National Energy Authority of Iceland
x State Electric Power Works of Iceland, Krafla Division

Approach

It should be emphasized that the modeling of a two-phase reservoir in its natural state is not a simple task. Simulations must be carried out for tens or hundreds of thousand years before steady state conditions are reached. Thus, these studies are very time consuming and incur substantial conputational expenses.

The Krafla field in its natural state is a dynamic system. However, the changes in thermodynamic conditions with time are probably very slow, so that a steady state approximation for the modeled reservoir system is reasonable.

The simulations reported below were carried out with Lawrence Berkeley Laboratory's general purpose simulator MULKOM (Pruess, 1982). Effects of non-condensible gases were neglected. A trial-and-error procedure is used, in which parameters of the reservoir model are initially fixed according to field data or estimates. Then the model is run until steady state is reached, and the resulting thermodynamic conditions and flows are compared with field observations. Model parameters are then modified until a satisfactory agreement with all relevant field information is obtained.

One question that arises in this procedure is, which of the field data should be used as model input, and which field data can be employed to check and confirm hypothetical assumptions and predictions of the model. We selected a small set of the most reliable field data as input, thereby avoiding to constrain the model by parameters of questionable accuracy. Most of the field data, which are known with less accuracy or confidence, can then be used as a check on calculated results.

Our reservoir model is a 1 m thick vertical section from west to east, which is based on the conceptual model in Figure 2. It extends from wells 5 and 7 in the west all the way to the impermeable fault zone between wells 17 and 18 in the east. The mesh design shown in Figure 3 is somewhat schematic, but preserves the main features and dimensions of the conceptual model. Surface discharge of steam in Hveragil and in the new wellfield is represented by appropriate sinks in elements 34, 44, 40 and 50. Influx areas and pressure boundary conditions are represented by boundary nodes B1 through B16 (Figure 3). Simulations were initialized with arbitrary thermodynamic conditions, but a possible dependence of the steady state on assumed initial conditions was investigated (see below).

Relative permeabilities were assumed to depend linearly on saturation, with immobile liquid and steam saturations of 0.30 and 0.05, respectively. While certainly not unique, this parametrization was shown to be consistent with individual well performance in Krafla (Pruess and Bodvarsson, to be published).

Best Model

After a lengthy process of trial and error we have obtained a model that represents very well the observed data on the natural state of the Krafla field. In the model we use 8 different regions that represent rocks with different material properties. The different regions are shown in Figure 4 and their material properties are given in Table 1. All of the regions are assumed to have the same values of rock density, heat capacity, and porosity. These parameters do not affect the results presented here, as steady state conditions do not depend upon storage-type parameters.

Regions 1 and 2 have low permeability, and represent a caprock and a confining layer, respectively. Region 3 is the average fracture/matrix material, the permeability of which was chosen according to the average value obtained from injection tests (Bodvarsson et. al., to be published). Regions 4 through 8 represent highly fractured zones, for whose existence and location there is direct evidence in the field.

The results for the steady state pressure distribution in the reservoir are shown in Figure 5. The figure shows that pressures are fairly uniform in the lower two-phase part of the reservoir. However, in the upper zone there are significant pressure differences at a given depth between the new and old wellfields. The 5-10 bar pressure difference compares well with field data. A comparison between observed and calculated pressure profiles for a typical well in the old wellfield is shown in Figure 6. The agreement is good, with slight differences most likely due to inaccurate measurements. The agreement between calculated and observed pressure profiles in the new field is similarly good.

The calculated temperature distribution in the system is shown in Figure 7. The figure shows that temperatures of 300°C are found at a depth of about 1000 m, and of over 340°C at a depth of 2000 m. At shallower depths the temperatures in the new wellfield are considerably higher than those in the upper reservoir in the old wellfield. This is due to boiling in the Hveragil fracture and the discharge of high enthalpy fluid to surface springs at Hveragil. The model shows that 0.00842 kg/s·m of high enthalpy vapor escapes to the surface at Hveragil. This compares very well with the value of 0.008 kg/s·m estimated by Armannsson and Gislason (personal communication, 1982). Similarly, the model indicates that 0.0023 kg/s·m of vapor feeds surface manifestations in the new wellfield, which

closely agrees with the estimated value of 0.003 kg/m·s.

The model shows excellent agreement with observed temperature profiles in the new wellfield. The comparison between observed and calculated temperature profiles in the old wellfield is not as good. Figure 8 shows temperature profiles for all wells in the old wellfield east of wells 5 and 7, as well as the calculated temperature profile in the old wellfield (broken line). The temperature gradients are highest in the low permeability caprock and the confining layer, where conduction dominates the heat transfer. There are two major discrepancies between the observed and calculated data. Firstly, the coarse mesh used in the simulations makes it impossible to accurately model the sharp break in the temperature profiles at a depth of 200 meters. The second difference is evident in the lower elements in the upper reservoir in the old wellfield. Field data indicate virtually isothermal conditions in the upper reservoir, whereas the calculated results show a 5-15°C difference in temperature between depths of 400 and 800 m. It is quite possible that the temperatures observed in wells do not accurately reflect formation temperatures. Our results are in agreement with hydrothermal alteration data, which indicate that the temperature in the upper reservoir should increase with depth (Stefansson, Kristmannsdottir, and Gislason, 1977). Furthermore, silica thermometer analysis of fluids from the upper reservoir shows temperatures of up to 240°C. It is also possible that the differences between observed and calculated temperatures may be due to the two-dimensional approximation employed in our model.

The steady state vapor saturation contours are shown in Figure 9. It should be emphasized that vapor saturations depend greatly on poorly known parameters such as relative permeabilities, so that the values shown in Figure 9 should be considered approximate. Also, the vapor saturations represent average values in the fracture system; vapor saturations in the rock matrix may be much lower. The figure shows that both the lower reservoir in the old wellfield and the reservoir in the new wellfield are under two-phase conditions. On the other hand the upper reservoir in the old wellfield is a compressed liquid reservoir. These observations agree with current notions about the reservoir. In general, most of the two-phase reservoir contains 10-20% of vapor by volume. The vapor saturation is higher in the upper part of both the lower reservoir in the old wellfield and the reservoir in the new wellfield. This is a result of upflow of steam from depth due to the nearly hydrostatic pressure gradient. It should be noted that infiltration of surface water (rainfall), which we have neglected, will tend to reduce vapor saturations in the upper parts of the reservoirs.

The steady state flow field in the reservoir system is shown in Figure 10. The arrows represent the total mass flow, i.e., the sum of the flows of the liquid and the vapor phase. Fluids enter the system from the west in the lower reservoir, and flow towards the east until they reach the high permeability upflow zone that intersects the surface at Hveragil. Most of the fluids from the upflow zone in the new wellfield rise until they reach the high permeability horizontal zone at a depth of 1000 m. The fluids then flow laterally along this fracture zone until they reach the Hveragil fracture, where the fluids from the old and the new wellfield mix. Some of the fluid mixture flows up the fault zone, and feeds surface manifestation at Hveragil, whereas the major portion recharges the upper reservoir at a rate of 0.013 kg/s·m. The results of the present model indicate that about 60% of the fluids come from the lower reservoir in the old wellfield and 40% from the upflow zone in the new wellfield. Geochemical data indicate that these mixing ratios are reasonable based on the chemical composition of the fluids from the different reservoirs (Gislason, personal communication, 1982).

It is of interest to note that fluid fluxes are largest (0.015 kg/s·m) in the Hveragil fault zone. This may indicate that wells intersecting this fault zone could be productive. Flow velocities are lowest in regions of low permeability and/or high vapor saturations, due to low mobilities of the fluids.

Sensitivity Studies

In order to check our natural state model of the Krafla reservoir, we have conducted sensitivity studies of many of the key model parameters. As mentioned earlier the steady state results obtained are not at all sensitive to storage-type parameters, such as porosity, rock density, and heat capacity. We will discuss the results only briefly due to the limited space available.

Permeability distribution

As a first example we consider the case of a homogeneous reservoir with a permeability of 2.0×10^{-15} m^2 (2mD), which is the average permeability inferred from analysis of injection tests of Krafla wells. The steady-state results showed too low pressures in the upper parts of the reservoirs when realistic pressures are applied at boundary nodes in the lower parts of the reservoirs. Using an anisotropy ratio of 5 (i.e., the vertical permeability is 5 times the horizontal permeability), reasonable pressures were obtained throughout the reservoir system. This seems to indicate that vertical fractures are very important fluid conduits in the Krafla reservoirs, and suggests that directional drilling may be more successful than conventional "straight-down" drilling. The steady-state flow field for the case of an anisotropy of 5 is shown in Figure 11.

Thermal Conductivities

For the reservoir model considered we find that convection is the dominant heat transfer mechanism. The convective heat loss to the surface springs is approximately 28700 W for the 1 m thick vertical section modeled. In comparison, the total heat loss through the caprock is only 1300 W, or only 5% of the convective heat losses. As a result, varying the thermal conductivity has relatively little effect on the steady-state thermodynamic conditions and fluid flows within the reservoir system, except in the upper reservoir in the old wellfield. Using a more detailed representation of the heat loss to the caprock we find that the best comparison with observed data is achieved when a thermal conductivity of 1.15 J/m·s·°C is used. The thermal conductivity of the confining layer is too insensitive a parameter to be determined with any accuracy.

Heat fluxes from below

The heat flux from below has a significant effect on steady state vapor saturations and pressures in the upper parts of the reservoir system. When the heat flux from below is neglected, a zone of single phase liquid results in the lower parts of the reservoir system. Similarly, when the heat flux is doubled from what we use in the best model (2.0 W/m^2), the pressures in the upper parts become too high due to higher vapor saturations and consequently greater upflow of steam.

Flow at surface springs

The fluid flow to the surface springs in Hveragil, extracted from elements 34 and 44, has major impact upon the temperature distribution in the upper reservoir. Consequently, the appropriate values were determined with good accuracy by the simulation. The flow to the surface springs in the new wellfield cannot be as accurately determined, but is within the range of 0.002 - 0.0027 $kg/s \cdot m$.

Relative permeabilities

In the base case (best model) we used linear relative permeability functions with immobile liquid and steam saturations of 0.30 and 0.05, respectively. An attempt was made to match the field data using the Corey relative permeability curves, with the same irreducible saturations. We found that the field data could not be matched using the Corey curves.

Uniqueness of steady-state solution

In the case of highly non-linear problems such as two-phase porous flow, there is always the question of uniqueness of the steady-state solution. In the simulations reported above we used initial conditions that resembled the observed data from the field (hot reservoir). In order to check on the uniqueness of the solution for the best model, we initialized a simulation with a "cold" reservoir, i.e. the temperatures of each layer were assigned values corresponding to a normal geothermal gradient (30°C/km). The results showed that after a lengthy transient heating period an identical steady-state solution was obtained. This provides evidence that the steady-state solutions using the best model may be unique.

Summary

The modeling of the natural state of the Krafla system has yielded results that closely match all available field data, and agree with a conceptual model developed from geochemical observations. Furthermore, studies of the sensitivity of various parameters give valuable insight into the permeabilities of different reservoir zones, thermal conductivity of the caprock, rates and enthalpies of natural recharge and discharge, and various other important reservoir parameters. The model presented here is two-dimensional, and only considers a part of the old wellfield. In the future, we hope to develop a natural-state model for the entire Krafla system, taking into account the three-dimensional nature of fluid flows.

Acknowledgement

The authors thank Sally Benson for a critical review of the manuscript. This research was performed as a part of a cooperative scientific investigation of the Krafla geothermal field between NEA, SEPW, ERI and SI of Iceland and LBL of U.S.A. This work was supported by SEPW of Iceland and the Assistant Secretary for Conservation and Renewable Energy, Office of Renewable Technology, Division of Geothermal and Hydropower Technologies of the U.S. Department of Energy under Contract No. DE-AC03-76SF00098.

References

Armannsson, H., Gislason, G. and T. Hauksson, Magmatic gases in wellfluids aid the mapping of the flow pattern in a geothermal system, Geochemica et Cosmochimica Acta, Vol. 46, pp. 167-177, 1982.

Pruess, K., Development of the general purpose simulator MULKOM, Annual Report 1982, Earth Sciences Division, Lawrence Berkeley Laboratory, Berkeley, Ca., 1982.

Stefansson, V., personal letter to G. S. Bodvarsson, April 1982.

Stefansson, V., Kristmannsdottir, H., and G. Gislason, Holubref 7, Orkustofnun, 1977.

Table 1: Material Properties of Reservoir Zones.

Zone	Density (kg/m^3)	Heat Capacity ($J/kg^\circ C$)	Thermal Cond. ($J/m.s.^\circ C$)	Porosity	Hor. Perm. (m^2)	Vert. Perm (m^2)
1	2650.	1000.	1.5	0.05	2×10^{-18}	2×10^{-18}
2	2650.	1000.	1.7	0.05	2×10^{-18}	2×10^{-18}
3	2650.	1000.	1.7	0.05	2×10^{-15}	2×10^{-15}
4	2650.	1000.	1.7	0.05	2×10^{-15}	3×10^{-14}
5	2650.	1000.	1.7	0.05	2×10^{-14}	2×10^{-15}
6	2650.	1000.	1.7	0.05	1×10^{-14}	2×10^{-15}
7	2650.	1000.	1.7	0.05	1×10^{-14}	3×10^{-14}
8	2650.	1000.	1.7	0.05	1×10^{-14}	2×10^{-14}

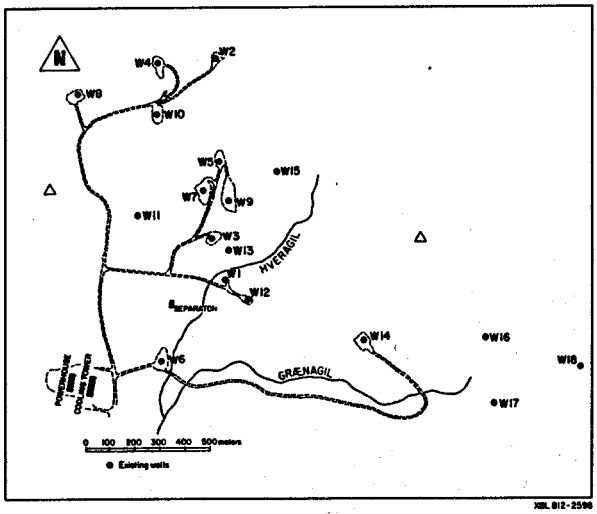

Figure 1: Well locations in Krafla field.

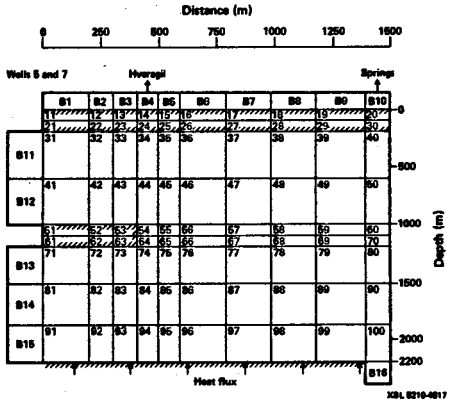

Figure 3: Simplified reservoir model and mesh used in the study of the natural state.

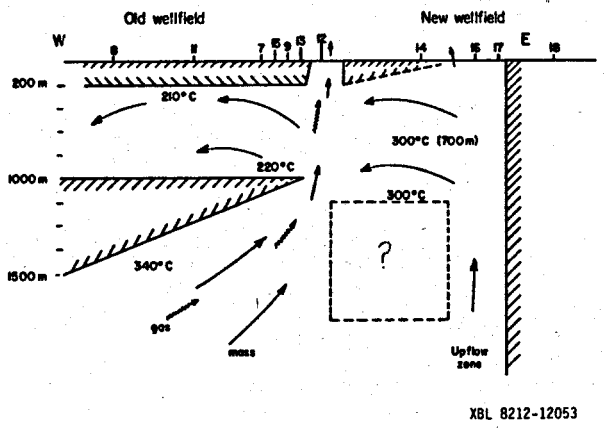

Figure 2: Conceptual model of the Krafla field.

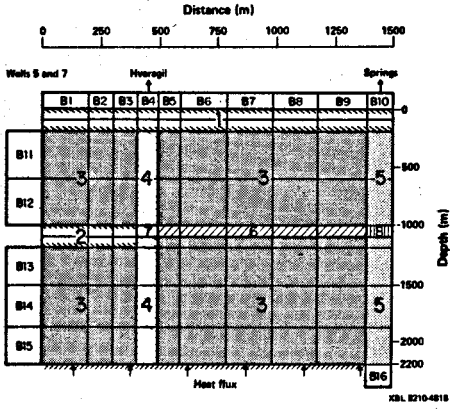

Figure 4: Different reservoir zones used in the best model.

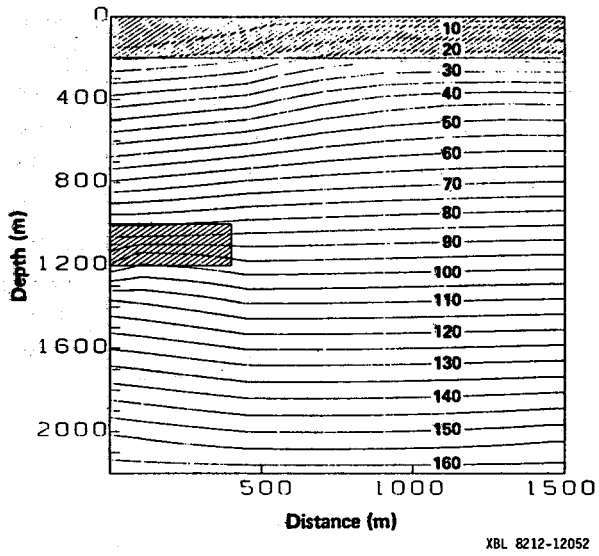

Figure 5: Steady-state pressure distribution in the natural state.

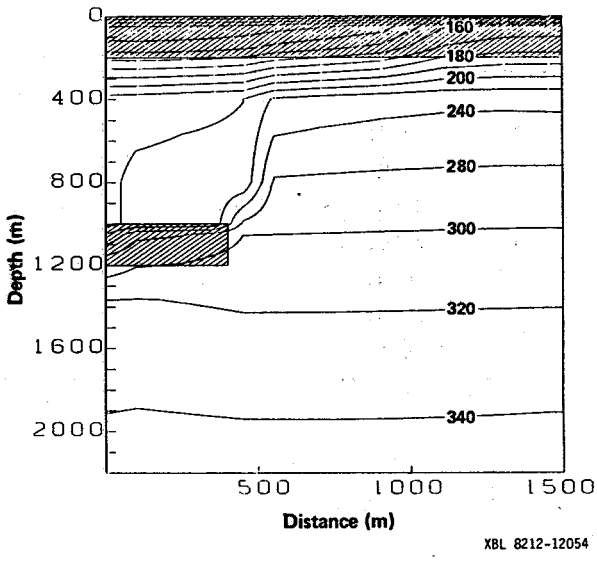

Figure 7: Steady-state temperature distribution in the natural state.

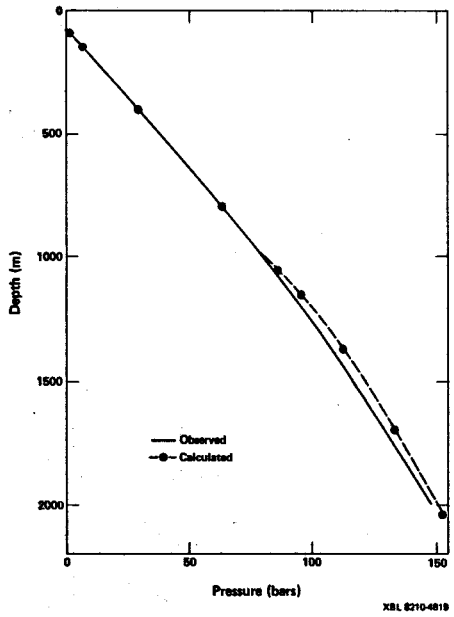

Figure 6: Comparison between observed and calculated pressure profiles in the old wellfield.

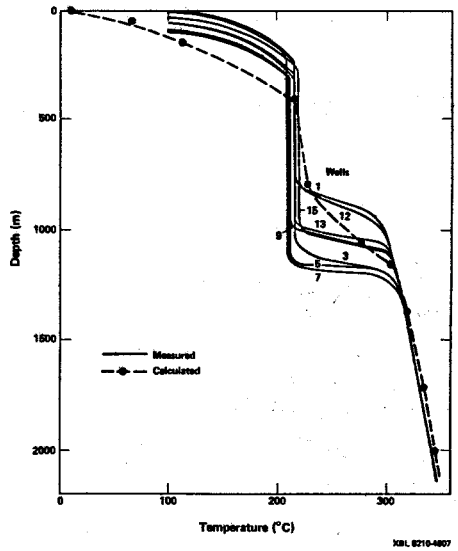

Figure 8: Comparison between observed and calculated temperature profiles in the old wellfield.

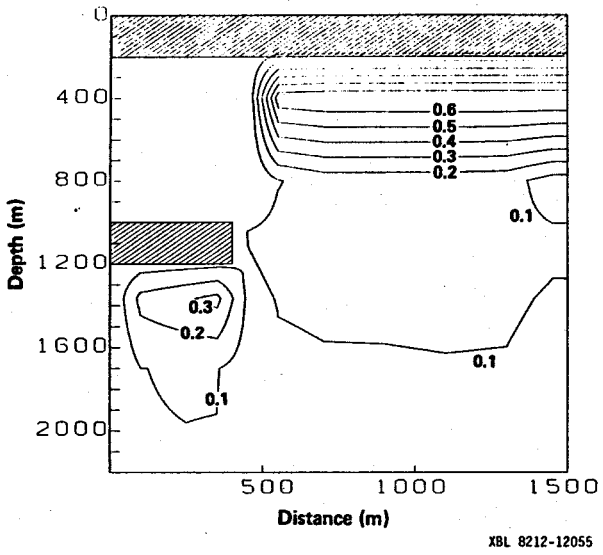

Figure 9: Steady-state vapor saturations in the natural state.

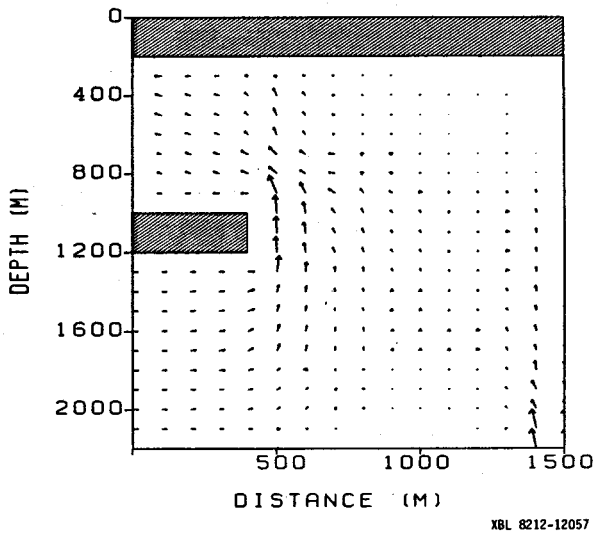

Figure 11: Steady-state flow field for the case of an anisotropy of 5.

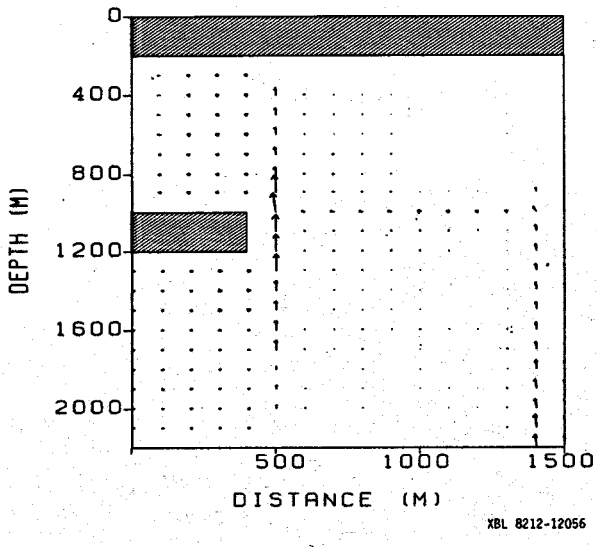

Figure 10: Steady-state flow field in the natural state (best case).